

International Journal of Modern Physics A
 © World Scientific Publishing Company

Magic square and Dirac flavor neutrino mass matrix

Yuta Hyodo

*Course of Physics, Graduate School of Science, Tokai University,
 4-1-1 Kitakaname, Hiratsuka, Kanagawa 259-1292, Japan
 0CSNM017@mail.u-tokai.ac.jp*

Teruyuki Kitabayashi

*Department of Physics, Tokai University,
 4-1-1 Kitakaname, Hiratsuka, Kanagawa 259-1292, Japan
 teruyuki@tokai-u.jp*

Received Day Month Year

Revised Day Month Year

The magic texture is one of the successful textures of the flavor neutrino mass matrix for the Majorana type neutrinos. The name “magic” is inspired by the nature of the magic square. We estimate the compatibility of the magic square with the Dirac, instead of the Majorana, flavor neutrino mass matrix. It turned out that some parts of the nature of the magic square are appeared approximately in the Dirac flavor neutrino mass matrix and the magic squares prefer the normal mass ordering rather than the inverted mass ordering for the Dirac neutrinos.

PACS numbers:14.60.Pq

1. Introduction

Understanding the nature of the flavor structure of elementary particles is one of the long-term problems in particle physics and cosmology.^{1,2} Many texture ansatz to solve the flavor puzzle are proposed, such as tri-bi maximal texture,^{3–5} texture zeros,^{6–41} $\mu - \tau$ symmetric texture^{42–62} and textures under A_n as well as S_n symmetries.⁶³

So-called *magic texture* is one of the textures of the flavor neutrino mass matrix for Majorana type neutrinos.^{64,65} The magic texture is parametrized as

$$M = \begin{pmatrix} a & b & c \\ b & d & a+c-d \\ c & a+c-d & b-c+d \end{pmatrix}. \quad (1)$$

The applications of the magic texture have been studied for texture zeros of flavor neutrino mass matrix,⁶⁶ with two simple extensions⁶⁷ and for baryon asymmetry of the Universe.⁶⁸

The name “magic” is inspired by the nature of the *magic square*.⁶⁹ A magic square of order n is a $n \times n$ square grid filled with distinct natural numbers. Each cell contains a number in the range $1, 2, \dots, n^2$. The sum of the numbers in each row, each column and diagonal is equal. For example, a magic square of order 3 is schematically shown as

$$\begin{array}{|c|c|c|} \hline 2 & 7 & 6 \\ \hline 9 & 5 & 1 \\ \hline 4 & 3 & 8 \\ \hline \end{array} \leftarrow 15 \quad \begin{array}{ccccc} \nearrow & \uparrow & \uparrow & \uparrow & \nwarrow \\ 15 & 15 & 15 & 15 & 15 \end{array} \quad (2)$$

where the sum (which is called magic constant or magic sum) is fifteen. The magic texture in Eq.(1) has a part of the nature of magic square, e.g., the sum of the elements in each row and each column is equal to $a + b + c$.

In this paper, we estimate the compatibility of the magic square with the Dirac, instead of the Majorana, flavor neutrino mass matrix by numerical calculations. We show that some parts of the nature of the magic square are appeared approximately in the Dirac flavor neutrino mass matrix. Moreover, as the main conclusion of this paper, we demonstrate that the magic squares prefer the normal mass ordering rather than the inverted mass ordering for the Dirac neutrinos.

This paper is organized as follows. In Section.2, four types of magic square are defined. In Section.3, the magic nature of the Dirac flavor neutrino mass matrix is estimated. Section 4 is devoted to a summary.

2. Classification

For a matrix

$$\begin{pmatrix} a & b & c \\ d & e & f \\ g & h & i \end{pmatrix} \leftarrow S_1 \quad \begin{array}{ccccc} \nearrow & \uparrow & \uparrow & \uparrow & \nwarrow \\ T' & S_4 & S_5 & S_6 & T \end{array} \quad (3)$$

we define the following eight sums

$$\begin{aligned} S_1 &= a + b + c, & S_2 &= d + e + f, & S_3 &= g + h + i, \\ S_4 &= a + d + g, & S_5 &= b + e + h, & S_6 &= c + f + i, \\ T &= a + e + i, & T' &= c + e + g, \end{aligned} \quad (4)$$

and the following four types of magic square in the from of the 3×3 matrix.

Type-I: The exact magic square (we call it type-I magic square) should satisfy the following requirement

$$S_1 = S_2 = S_3 = S_4 = S_5 = S_6 = T = T'. \quad (5)$$

In this case, the standard deviation should vanish:

$$sd_I = \sqrt{\frac{\sum_{i=1}^6 (S_i - \bar{S})^2 + (T - \bar{S})^2 + (T' - \bar{S})^2}{8}}, \quad (6)$$

where

$$\bar{S} = (S_1 + S_2 + S_3 + S_4 + S_5 + S_6 + T + T')/8, \quad (7)$$

is the average of the sums S_1, S_2, \dots, S_6, T and T' . For example, in the case of order 3 magic square

$$\begin{pmatrix} 2 & 7 & 6 \\ 9 & 5 & 1 \\ 4 & 3 & 8 \end{pmatrix}, \quad (8)$$

the sums

$$S_1 = S_2 = S_3 = S_4 = S_5 = S_6 = T = T' = 15, \quad (9)$$

and the average $\bar{S} = 15$ are obtained and the standard deviation becomes $sd_I = 0$. Moreover, we obtain the vanishing standard deviation for the following decimal magic square:

$$\begin{pmatrix} 0.2 & 0.7 & 0.6 \\ 0.9 & 0.5 & 0.1 \\ 0.4 & 0.3 & 0.8 \end{pmatrix}. \quad (10)$$

In deed, the sums of this decimal magic square

$$S_1 = S_2 = S_3 = S_4 = S_5 = S_6 = T = T' = 1.5, \quad (11)$$

and the average $\bar{S} = 1.5$ are obtained and the standard deviation becomes $sd_I = 0$.

The standard deviation sd_I is a good number to show that whether a matrix has the nature of the exact type-I magic square or not; however, the standard deviation is not good number for our purpose in this paper. For example, the matrix

$$\begin{pmatrix} 2+1 & 7 & 6 \\ 9 & 5 & 1 \\ 4 & 3 & 8 \end{pmatrix}, \quad (12)$$

and

$$\begin{pmatrix} 0.2+0.1 & 0.7 & 0.6 \\ 0.9 & 0.5 & 0.1 \\ 0.4 & 0.3 & 0.8 \end{pmatrix}, \quad (13)$$

have a small perturbation for the type-I magic square in the (1,1) element. Because the requirement of the type-I magic square is only the relation of $S_1 = S_2 = S_3 = S_4 = S_5 = S_6 = T = T'$, these two matrices are same level of type-I magic square; however, the standard deviations of the matrices in Eq.(12) and Eq.(13) are 0.484 and 0.0484, respectively.

We define the *magic index* for the type-I magic square as follows

$$s_I = \sqrt{\frac{\sum_{i=1}^6 (\frac{S_i}{S} - 1)^2 + (\frac{T}{S} - 1)^2 + (\frac{T'}{S} - 1)^2}{8}}. \quad (14)$$

The magic index s_I of the matrices in Eq.(12) and Eq.(13) are same as 0.0315.

The small magic index for a matrix means the matrix is much compatible with the magic square.

Type-II: If we relax the requirement of the exact magic square in Eq.(5), we can define the quasi-magic squares. Omitting the trace T in the exact magic requirement in Eq.(5), we have a new requirement

$$S_1 = S_2 = S_3 = S_4 = S_5 = S_6 = T', \quad (15)$$

for a matrix. We call a matrix with the requirement of Eq.(15) the type-II magic square. For the type-II magic square, we define the following magic index

$$s_{II} = \sqrt{\frac{\sum_{i=1}^6 (\frac{S_i}{S} - 1)^2 + (\frac{T'}{S} - 1)^2}{7}}, \quad (16)$$

where

$$\bar{S} = (S_1 + S_2 + S_3 + S_4 + S_5 + S_6 + T')/7. \quad (17)$$

Type-III: Omitting the sum T' in the exact magic constraint in Eq.(5), we have other new requirement

$$S_1 = S_2 = S_3 = S_4 = S_5 = S_6 = T, \quad (18)$$

for a matrix. We call a matrix with the requirement of Eq.(18) the type-III magic square and we define the following type-III magic index

$$s_{III} = \sqrt{\frac{\sum_{i=1}^6 (\frac{S_i}{S} - 1)^2 + (\frac{T}{S} - 1)^2}{7}}, \quad (19)$$

where

$$\bar{S} = (S_1 + S_2 + S_3 + S_4 + S_5 + S_6 + T)/7. \quad (20)$$

Type-IV: Finally, we define the type-IV magic square by omitting the sum T' and trace T in the exact magic requirement in Eq.(5). In this case, the requirement becomes

$$S_1 = S_2 = S_3 = S_4 = S_5 = S_6, \quad (21)$$

and we define the following type-IV magic index

$$s_{IV} = \sqrt{\frac{\sum_{i=1}^6 (\frac{S_i}{S} - 1)^2}{6}}, \quad (22)$$

where

$$\bar{S} = (S_1 + S_2 + S_3 + S_4 + S_5 + S_6)/6. \quad (23)$$

We note that the type-IV magic square is a Dirac neutrino version of the magic texture for Majorana neutrinos in Eq.(1).

3. Magic square and Dirac neutrino mass matrix

In this section, first, we show the brief review of the Dirac neutrino mass matrix and the experimental data of the neutrinos. Then, we estimate the compatibility of the magic square with the Dirac flavor neutrino mass matrix by numerical calculations.

3.1. Neutrino mass matrix

The minimal flavor neutrino mass matrix for Dirac neutrinos is obtained by⁷⁰

$$M = \begin{pmatrix} M_{ee} & M_{e\mu} & M_{e\tau} \\ M_{\mu e} & M_{\mu\mu} & M_{\mu\tau} \\ M_{\tau e} & M_{\tau\mu} & M_{\tau\tau} \end{pmatrix} = \begin{pmatrix} U_{e1}m_1 & U_{e2}m_2 & U_{e3}m_3 \\ U_{\mu 1}m_1 & U_{\mu 2}m_2 & U_{\mu 3}m_3 \\ U_{\tau 1}m_1 & U_{\tau 2}m_2 & U_{\tau 3}m_3 \end{pmatrix}, \quad (24)$$

where m_1, m_2 and m_3 denote the neutrino mass eigenstates and

$$\begin{aligned} U_{e1} &= c_{12}c_{13}, & U_{e2} &= s_{12}c_{13}, & U_{e3} &= s_{13}e^{-i\delta}, \\ U_{\mu 1} &= -s_{12}c_{23} - c_{12}s_{23}s_{13}e^{i\delta}, \\ U_{\mu 2} &= c_{12}c_{23} - s_{12}s_{23}s_{13}e^{i\delta}, & U_{\mu 3} &= s_{23}c_{13}, \\ U_{\tau 1} &= s_{12}s_{23} - c_{12}c_{23}s_{13}e^{i\delta}, \\ U_{\tau 2} &= -c_{12}s_{23} - s_{12}c_{23}s_{13}e^{i\delta}, & U_{\tau 3} &= c_{23}c_{13}, \end{aligned} \quad (25)$$

denote the elements of the Pontecorvo-Maki-Nakagawa-Sakata mixing matrix.⁷¹⁻⁷⁴ We used the abbreviations $c_{ij} = \cos \theta_{ij}$ and $s_{ij} = \sin \theta_{ij}$ ($i, j = 1, 2, 3$). The Dirac CP phase is denoted by δ .

A global analysis of current data shows the following the best-fit values of the squared mass differences $\Delta m_{ij}^2 = m_i^2 - m_j^2$ and the mixing angles for the so-called normal mass ordering (NO), $m_1 < m_2 < m_3$, of the neutrinos:⁷⁵

$$\begin{aligned} \frac{\Delta m_{21}^2}{10^{-5}\text{eV}^2} &= 7.39_{-0.20}^{+0.21} \quad (6.79 \rightarrow 8.01), \\ \frac{\Delta m_{31}^2}{10^{-3}\text{eV}^2} &= 2.528_{-0.031}^{+0.029} \quad (2.436 \rightarrow 2.618), \\ \theta_{12}/^\circ &= 33.82_{-0.76}^{+0.78} \quad (31.61 \rightarrow 36.27), \\ \theta_{23}/^\circ &= 48.6_{-1.4}^{+1.0} \quad (41.1 \rightarrow 51.3), \\ \theta_{13}/^\circ &= 8.60_{-0.13}^{+0.13} \quad (8.22 \rightarrow 8.98), \\ \delta/^\circ &= 221_{-28}^{+39} \quad (144 \rightarrow 357), \end{aligned} \quad (26)$$

where the \pm denotes the 1σ region and the parentheses denote the 3σ region. On the other hands, for the so-called inverted mass ordering, $m_3 < m_1 \lesssim m_2$, we have

$$\begin{aligned} \frac{\Delta m_{21}^2}{10^{-5}\text{eV}^2} &= 7.39^{+0.21}_{-0.20} \quad (6.79 \rightarrow 8.01), \\ \frac{\Delta m_{32}^2}{10^{-3}\text{eV}^2} &= -2.510^{+0.030}_{-0.031} \quad (-2.601 \rightarrow -2.416), \\ \theta_{12}/^\circ &= 33.82^{+0.78}_{-0.75} \quad (31.61 \rightarrow 36.27), \\ \theta_{23}/^\circ &= 48.4^{+1.0}_{-1.2} \quad (41.4 \rightarrow 51.3), \\ \theta_{13}/^\circ &= 8.64^{+0.12}_{-0.13} \quad (8.26 \rightarrow 9.02), \\ \delta/^\circ &= 282^{+23}_{-25} \quad (205 \rightarrow 348). \end{aligned} \quad (27)$$

Moreover, the following constraints

$$\sum m_i < 0.12 - 0.69 \text{ eV}, \quad (28)$$

from the cosmological observation of the cosmic microwave background radiation^{39, 76–79} as well as

$$|M_{ee}| < 0.066 - 0.155 \text{ eV}, \quad (29)$$

from the neutrino less double beta decay experiments^{39, 80} are obtained.

3.2. Numerical analysis

To estimate the compatibility of the magic square with the Dirac flavor neutrino mass matrix by numerical calculations, we employ the following real matrix

$$\begin{pmatrix} a & b & c \\ d & e & f \\ g & h & i \end{pmatrix} = \begin{pmatrix} |M_{ee}| & |M_{e\mu}| & |M_{e\tau}| \\ |M_{\mu e}| & |M_{\mu\mu}| & |M_{\mu\tau}| \\ |M_{\tau e}| & |M_{\tau\mu}| & |M_{\tau\tau}| \end{pmatrix}, \quad (30)$$

instead of the complex Dirac mass matrix in Eq.(24).

In our numerical calculation, we require that the square mass differences Δm_{ij}^2 , mixing angles θ_{ij} and the Dirac CP violating phase δ are varied within the 3σ experimental ranges and the lightest neutrino mass is varied within $0.001 - 0.1$ eV. We also require that the constraints $|M_{ee}| < 0.155$ eV and $\sum m_i < 0.241$ eV (TT, TE, EE+LowE+lensing^{40, 76}) are satisfied.

We show the results from the numerical calculations in Tables 1 - 3 as well as Figures 1 and 2.

Table 1 shows that the minimum and maximum values of the magic indices of type-I, -II, -III and type-IV magic squares for the Dirac flavor neutrino mass matrix. We recall that the small magic index for a matrix means the matrix is much compatible with the magic square. We note the following three points:

- The top row in the Table 1 shows that the minimum of the type-I magic index are $s_1^{\min} = 0.132$ and $s_1^{\min} = 0.136$ for NO and IO, respectively. Thus,

Table 1. Minimum and maximum values of magic index.

type	magic index	NO	IO
I	s_I^{\min}	0.132	0.136
	s_I^{\max}	0.783	0.462
II	s_{II}^{\min}	0.102	0.107
	s_{II}^{\max}	0.874	0.504
III	s_{III}^{\min}	0.0729	0.0956
	s_{III}^{\max}	0.739	0.476
IV	s_{IV}^{\min}	0.0593	0.0888
	s_{IV}^{\max}	0.832	0.525

Table 2. The sums $S_1, S_2, \dots, S_6, T, T'$ of the type-I, -II, -III and type-IV magic squares for the Dirac flavor neutrino mass matrix in the unit of eV. The upper (lower) half of the table shows the sums in the case of NO (IO). For each type of magic squares, the upper (lower) row shows the sums for s_{\min} (s_{\max}).

NO									
type	s	S_1	S_2	S_3	S_4	S_5	S_6	T'	T
I	s_I^{\min}	0.117	0.133	0.139	0.120	0.130	0.138	0.0971	0.158
	s_I^{\max}	0.0128	0.0387	0.0433	0.00166	0.0144	0.0788	0.0126	0.0436
II	s_{II}^{\min}	0.117	0.135	0.137	0.122	0.129	0.139	0.100	-
	s_{II}^{\max}	0.0129	0.0383	0.0432	0.00168	0.0145	0.0782	0.0123	-
III	s_{III}^{\min}	0.118	0.137	0.136	0.123	0.129	0.139	-	0.149
	s_{III}^{\max}	0.0129	0.0387	0.0432	0.00163	0.0144	0.0788	-	0.0434
IV	s_{IV}^{\min}	0.118	0.137	0.136	0.123	0.129	0.139	-	-
	s_{IV}^{\max}	0.0127	0.0389	0.0432	0.00166	0.0144	0.0788	-	-
IO									
type	s	S_1	S_2	S_3	S_4	S_5	S_6	T'	T
I	s_I^{\min}	0.129	0.126	0.138	0.137	0.148	0.107	0.105	0.160
	s_I^{\max}	0.0677	0.0451	0.0529	0.0798	0.0843	0.00156	0.0406	0.0619
II	s_{II}^{\min}	0.128	0.132	0.133	0.138	0.147	0.109	0.107	-
	s_{II}^{\max}	0.0694	0.0462	0.0543	0.0820	0.0864	0.00155	0.0414	-
III	s_{III}^{\min}	0.128	0.131	0.134	0.140	0.146	0.108	-	0.150
	s_{III}^{\max}	0.0683	0.0429	0.0559	0.0782	0.0873	0.00158	-	0.0723
IV	s_{IV}^{\min}	0.127	0.133	0.132	0.137	0.147	0.109	-	-
	s_{IV}^{\max}	0.0677	0.0430	0.0552	0.0777	0.0865	0.00163	-	-

the exact magic square (type-I magic square) is hardly realized for the Dirac flavor neutrino mass matrix.

- The smallest minimum magic index for NO(IO) is obtained in the case of type-IV as 0.0593 (0.0888). Thus, if we relax the requirement of the magic squares from exact magic square (type-I) to relatively rough magic square (type-IV), some parts of the nature of the magic square are appeared for the Dirac flavor neutrino mass matrix.
- The magic squares prefer the normal mass ordering rather than the inverted mass ordering.

Table 2 shows the sums $S_1, S_2, \dots, S_6, T, T'$ of the type-I, -II, -III and type-IV magic squares for the Dirac flavor neutrino mass matrix in the unit of eV. The

Table 3. The neutrino parameters m_i, θ_{ij}, δ of the type-I, -II, -III and type-IV magic squares for the Dirac flavor neutrino mass matrix. The upper (lower) half of the table shows the sums in the case of NO (IO). For each type of magic squares, the upper (lower) row shows the sums for s_{\min} (s_{\max})

NO								
type	s	m_1 [eV]	m_2 [eV]	m_3 [eV]	$\theta_{12}/^\circ$	$\theta_{23}/^\circ$	$\theta_{13}/^\circ$	$\delta/^\circ$
I	s_I^{\min}	0.0745	0.0750	0.0897	36.12	51.19	8.851	183.9
	s_I^{\max}	0.00104	0.00834	0.0511	33.14	41.39	8.400	345.7
II	s_{II}^{\min}	0.0746	0.0750	0.0894	35.56	41.17	8.964	181.4
	s_{II}^{\max}	0.00105	0.00838	0.0507	34.92	41.12	8.270	345.9
III	s_{III}^{\min}	0.0748	0.0754	0.0899	36.20	51.10	8.866	340.2
	s_{III}^{\max}	0.00101	0.00832	0.0511	35.43	41.48	8.277	336.7
IV	s_{IV}^{\min}	0.0751	0.0756	0.0899	35.88	51.17	8.980	354.5
	s_{IV}^{\max}	0.00104	0.00832	0.0512	32.88	41.51	8.294	325.1
IO								
type	s	m_1 [eV]	m_2 [eV]	m_3 [eV]	$\theta_{12}/^\circ$	$\theta_{23}/^\circ$	$\theta_{13}/^\circ$	$\delta/^\circ$
I	s_I^{\min}	0.0852	0.0856	0.0691	36.21	51.20	8.982	205.1
	s_I^{\max}	0.0487	0.0494	0.00101	35.50	51.08	8.619	343.9
II	s_{II}^{\min}	0.0852	0.0856	0.0701	33.23	41.41	8.881	205.3
	s_{II}^{\max}	0.0500	0.0506	0.00101	35.66	51.10	8.822	347.4
III	s_{III}^{\min}	0.0851	0.0855	0.0699	35.74	50.98	8.947	343.5
	s_{III}^{\max}	0.0498	0.0506	0.00102	31.62	51.16	8.594	210.3
IV	s_{IV}^{\min}	0.0852	0.0857	0.0701	32.25	48.50	8.906	329.1
	s_{IV}^{\max}	0.0494	0.0500	0.00106	32.14	50.68	8.959	208.5

upper (lower) half of the Table 2 shows the sums in the case of NO (IO). For each type of magic squares, the upper (lower) row shows the sums for s_{\min} (s_{\max}). We note the following point:

- The sum of the diagonal elements T' or T tends to differ from other sums in the type-I and type-II. This character of T' or T yields the large magic index (deviation from the magic square).

Table 3 shows the neutrino parameters m_i, θ_{ij}, δ of the type-I, -II, -III and type-IV magic squares for the Dirac flavor neutrino mass matrix. As same as Table 2, the upper (lower) half of the Table 3 shows the sums in the case of NO (IO). For each type of magic squares, the upper (lower) row shows the sums for s_{\min} (s_{\max}). The following ranges of the neutrino parameters are roughly favored for the magic squares:

$$\begin{aligned}
 m_i/\text{eV} &\sim 0.07 - 0.09, \\
 \theta_{12}/^\circ &\sim 36, \\
 \theta_{23}/^\circ &\sim 51, (\text{for type - I, -III, -IV}), \quad \sim 41, (\text{for type - II}), \\
 \theta_{13}/^\circ &\sim 8.9 \\
 \delta/^\circ &\sim 181 - 184, (\text{for type - I, -II}), \quad \sim 340, (\text{for type - III, IV}),
 \end{aligned} \tag{31}$$

for NO and

$$\begin{aligned}
 m_i/\text{eV} &\sim 0.07 - 0.09, \\
 \theta_{12}/^\circ &\sim 33 - 36, \\
 \theta_{23}/^\circ &\sim 51, (\text{for type - I, -III, -IV}), \quad \sim 41, (\text{for type - II}), \\
 \theta_{13}/^\circ &\sim 8.9 \\
 \delta/^\circ &\sim 205, (\text{for type - I, -II}), \quad \sim 329 - 344, (\text{for type - III, IV}),
 \end{aligned} \tag{32}$$

for IO.

Figure 1 and Figure 2 show that the dependence of the neutrino parameters m_i, θ_{ij}, δ on the magic index s in the case of NO and IO, respectively. We note the following four points:

- The large neutrino masses yield small magic indices (the large masses are favorable for magic squares).
- The minimum of s_I , s_{II} and s_{III} for type-I, -II and -III are obtained with large θ_{12} , θ_{23} and θ_{13} .
- The minimum of s_I and s_{II} for type-I and type-II are obtained with small δ .
- The minimum of s_{III} for type-III is obtained with large δ .

for both NO and IO.

We would like to emphasize again the following remarkable result of our numerical calculations:

- All types of the magic squares prefer the normal mass ordering rather than the inverted mass ordering (see Table 1).

Although the neutrino mass ordering (either NO or IO) is not determined experimentaly, a global analysis shows that the preference for the normal mass ordering is mostly due to neutrino oscillation measurements.^{39,81,82} The theoretical origin of the mass ordering of neutrinos is still big problem. There is a possibility that the origin of the normal mass ordering is the magic nature of the neutrinos.

10 Yuta Hyodo

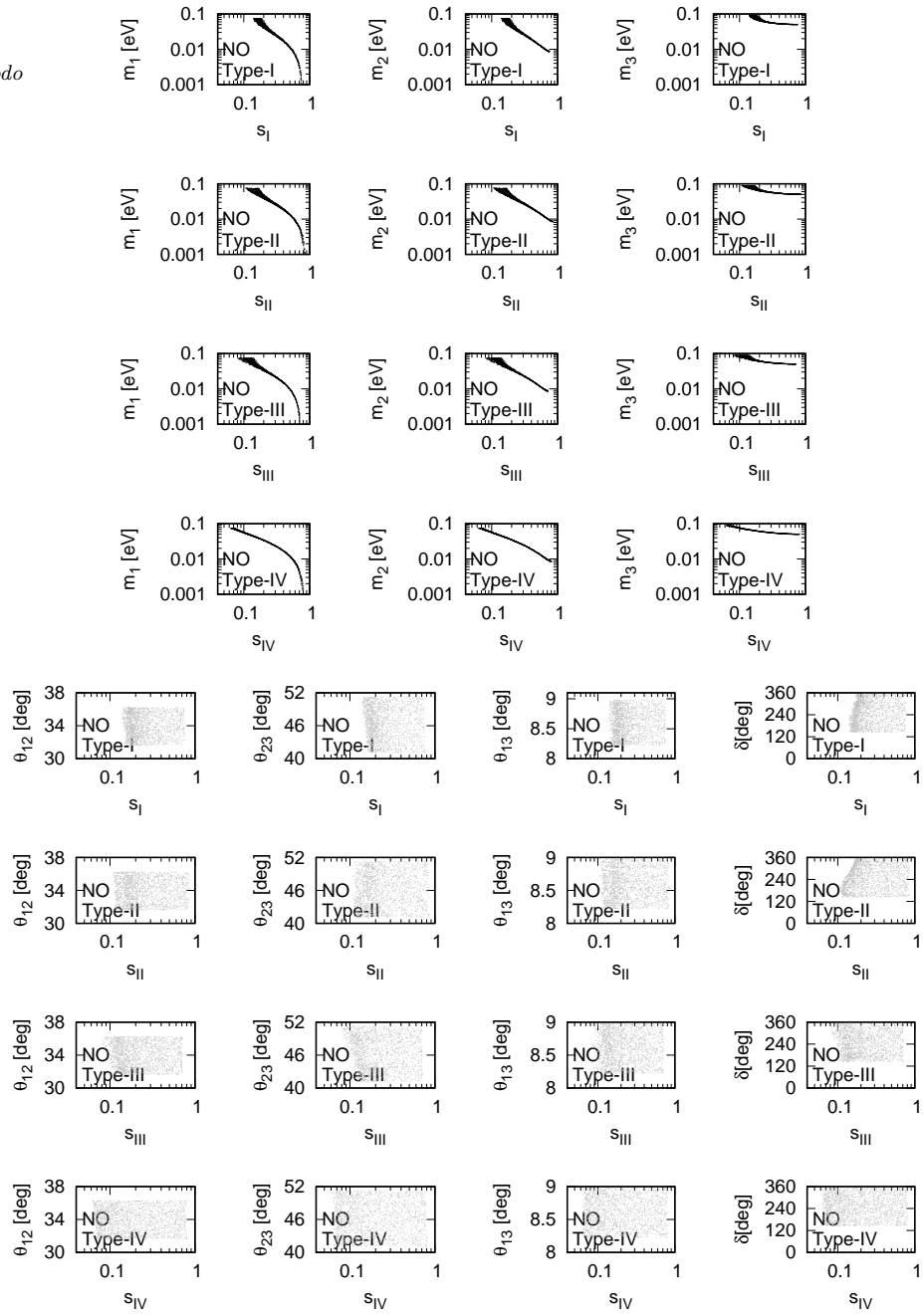


Fig. 1. Dependence of the neutrino parameters \$m_i, \theta_{ij}, \delta\$ on the magic index \$s\$ in the case of NO.

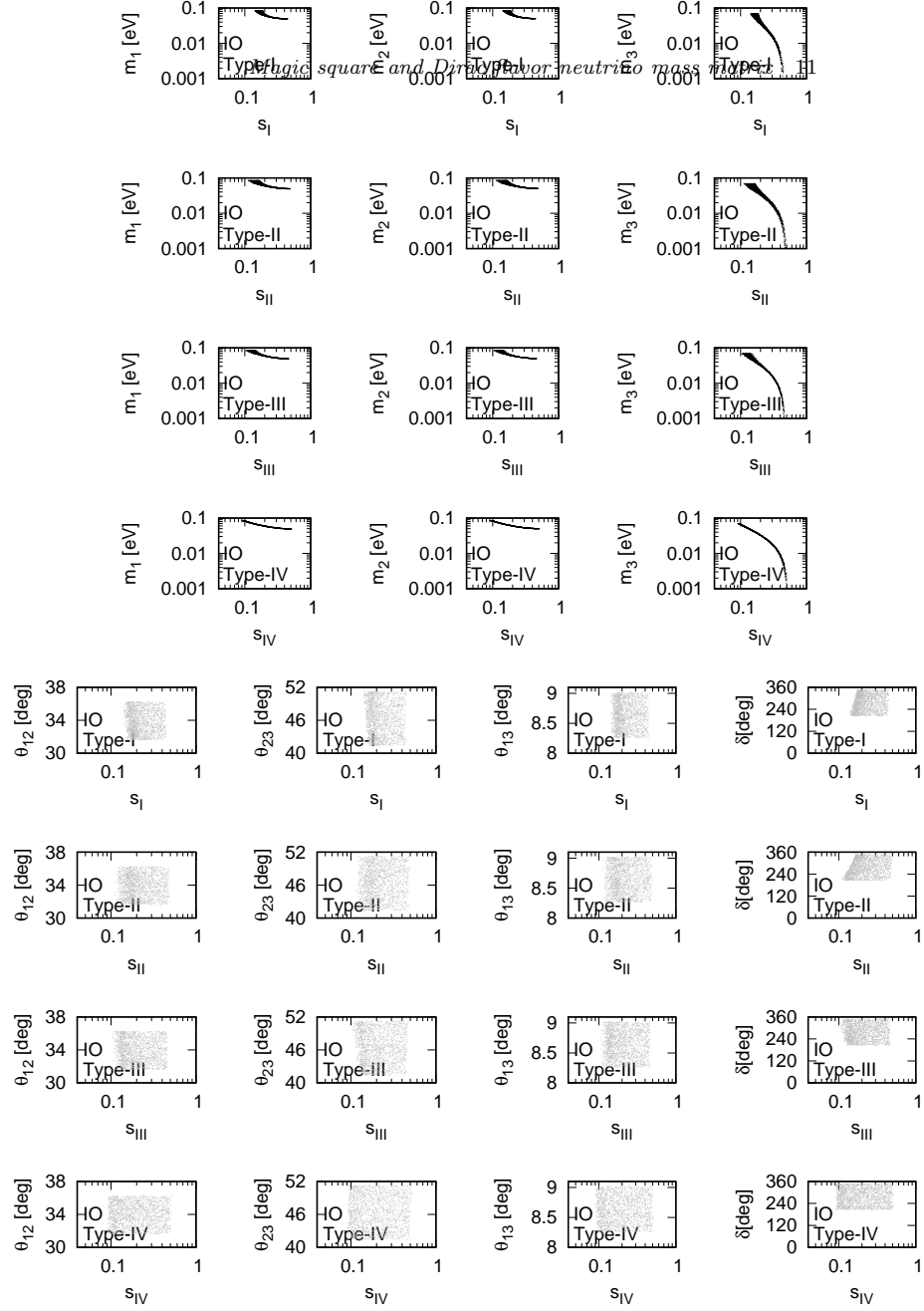


Fig. 2. Same as Figure 1 but in the case of IO.

4. Summary

The magic texture is one of the successful textures of the flavor neutrino mass matrix for the Majorana type neutrinos. The name “magic” is inspired by the nature of the magic square. In this paper, we have estimated the compatibility of the magic square with the Dirac, instead of the Majorana, flavor neutrino mass matrix by numerical calculations. We have shown that some parts of the nature of the magic square are appeared approximately in the Dirac flavor neutrino mass matrix and the magic squares prefer the normal mass ordering rather than the inverted mass ordering for the Dirac neutrinos.

Finally, we would like to comment about Eq.(30). In this paper, we have estimated the compatibility of the magic square with the real matrix in Eq.(30) instead of the complex Dirac mass matrix in Eq.(24). This approach may be enough as a first step of the study about the relation between the magic square and the Dirac flavor neutrino mass matrix; however, if we estimate the compatibility of the magic square with the complex Dirac mass matrix in Eq.(24) by an appropriate method, the results may be modified. A detailed analysis of this topic will be found in our future study.

References

1. S. F. King, J. Phys. G **42**, 123001 (2015).
2. F. Feruglio and A. Romanino, “Neutrino Flavour Symmetries”, arXiv:1912.06028 (Dec 2019).
3. P. F. Harrison, D. H. Perkins, and W. G. Scott, Phys. Lett. B **530**, 167 (2002).
4. Z. -z. Xing, Phys. Lett. B **533**, 85 (2002).
5. P. F. Harrison and W. G. Scott, Phys. Lett. B **535**, 163 (2002).
6. M. S. Berger and K. Siyeon, Phys. Rev. D **64**, 053006 (2001).
7. P. H. Frampton, S. L. Glashow, and D. Marfatia, Phys. Lett. B **536**, 79 (2002).
8. Z. -z. Xing, Phys. Lett. B **530**, 159 (2002).
9. Z. -z. Xing, Phys. Lett. B **539**, 85 (2002).
10. A. Kageyama, S. Kaneko, N. Shimoyana, and M. Tanimoto, Phys. Lett. B **538**, 96 (2002).
11. Z. -z. Xing, Phys. Rev. D **69**, 013006 (2004).
12. W. Grimus, A. S. Joshipura, L. Lavoura, and M. Tanimoto, Eur. Phys. J. C **36**, 227 (2004).
13. C. I. Low, Phys. Rev. D **70**, 073013 (2004).
14. C. I. Low, Phys. Rev. D **71**, 073007 (2005).
15. W. Grimus and L. Lavoura, J. Phys. G **31**, 693 (2005).
16. S. Dev, S. Kumar, S. Verma, and S. Gupta, Phys. Rev. D **76**, 013002 (2007).
17. Z. -z. Xing and S. Zhou, Phys. Lett. B **679**, 249 (2009).
18. H. Fritzsch, Z. -z. Xing, and S. Zhou, J. High Energy Phys. **09**, 083 (2011).
19. S. Kumar, Phys. Rev. D **84**, 077301 (2011).
20. S. Dev, S. Gupta, and R. R. Gautam, Phys. Lett. B **701**, 605 (2011).
21. T. Araki, J. Heeck, and J. Kubo, J. High Energy Phys. **07**, 083 (2012).
22. P. Ludle, S. Morisi, and E. Peinado, Nucl. Phys. B **857**, 411 (2012).
23. E. Lashin and N. Chamoun, Phys. Rev. D **85**, 113011 (2012).

24. K. Deepthi, S. Gollu, and R. Mohanta, Eur. Phys. J. C **72**, 1888 (2012).
25. D. Meloni and G. Blankenburg, Nucl. Phys. B **867**, 749 (2013).
26. D. Meloni, A. Meroni, and E. Peinado, Phys. Rev. D **89**, 053009 (2014).
27. S. Dev, R. R. Gautam, L. Singh, and M. Gupta, Phys. Rev. D **90**, 013021 (2014).
28. R. G. Felipe and H. Serodio, Nucl. Phys. B **886**, 75 (2014).
29. P. O. Ludl and W. Grimus, J. High Energy Phys. **07**, 090 (2014).
30. L. M. Cebola, D. E. Costa, and R. G. Felipe, Phys. Rev. D **92**, 025005 (2015).
31. R. R. Gautam, M. Singh, and M. Gupta, Phys. Rev. D **92**, 013006 (2015).
32. S. Dev, L. Singh, and D. Raj, Eur. Phys. J. C **75**, 394 (2015).
33. T. Kitabayashi and M. Yasuè, Phys. Rev. D **93**, 053012 (2016).
34. S. Zhou, Chin. Phys. C **40**, 033102 (2016).
35. M. Singh, G. Ahuja and M. Gupta, Prog. Theor. Exp. Phys. **2016**, 123B08 (2016).
36. K. Bora, D. Borah and D. Dutta, Phys. Rev. D **96**, 075006 (2017).
37. D. M. Barreiros, R. G. Felipe and F. R. Joaquim, Phys. Rev. D **97**, 115016 (2018).
38. D. M. Barreiros, R. G. Felipe and F. R. Joaquim, J. High Energy Phys. **01**, 223 (2019).
39. F. Capozzi, E. D. Valentino and E. Lisi, A. Marrone, A. Melchiorri and A. Palazzo, Phys. Rev. D **101**, 116013 (2020).
40. M. Singh, EPL **2020**, 11002 (2020).
41. D. M. Barreiros, F. R. Joaquim and T. T. Yanagida, arXiv:2003.06332.
42. T. Fukuyama and H. Nishiura, (1997), arXiv:hep-ph/9702253.
43. C. S. Lam, Phys. Lett. B **507**, 214 (2001).
44. E. Ma and M. Raidal, Phys. Rev. Lett. **87**, 011802 (2001); Erratum Phys. Rev. Lett. **87**, 159901 (2001).
45. K. R. S. Balaji, W. Grimus, and T. Schwetz, Phys. Lett. B **508**, 301 (2001).
46. Y. Koide, H. Nishiura, K. Matsuda, T. Kikuchi, and T. Fukuyama, Phys. Rev. D **66**, 093006 (2002).
47. T. Kitabayashi and M. Yasue, Phys. Rev. D **67**, 015006 (2003).
48. Y. Koide, Phys. Rev. D **69**, 093001 (2004).
49. I. Aizawa, M. Ishiguro, T. Kitabayashi, and M. Yasue, Phys. Rev. D **70**, 015011 (2004).
50. A. Ghosal, Mod. Phys. Lett. A **19**, 2579 (2004).
51. R. N. Mohapatra and W. Rodejohann, Phys. Rev. D **72**, 053001 (2005).
52. Y. Koide, Phys. Lett. B **607**, 123 (2005).
53. T. Kitabayashi and M. Yasue, Phys. Lett. B **621**, 133 (2005).
54. N. Haba and W. Rodejohann, Phys. Rev. D **74**, 017701 (2006).
55. Z.-z. Xing, H. Zhang, and S. Zhou, Phys. Lett. B **641**, 189 (2006).
56. Y. H. Ahn, S. K. Kang, C. S. Kim, and J. Lee, Phys. Rev. D **73**, 093005 (2006).
57. A. S. Joshipura, Eur. Phys. J. C **53**, 77 (2008).
58. J. C. Gomez-Izquierdo and A. Perez-Lorenzana, Phys. Rev. D **82**, 033008 (2010).
59. H.-J. He and F.-R. Yin, Phys. Rev. D **84**, 033009 (2011).
60. H.-J. He and X.-J. Xu, Phys. Rev. D **86**, 111301 (2012).
61. J. C. Gomez-Izquierdo, Eur. Phys. J. C **77**, 551 (2017).
62. T. Fukuyama, Prog. Theor. Exp. Phys. **2017**, 033B11 (2017).
63. G. Altarelli and F. Feruglio, Rev. Mod. Phys. **82**, 2701 (2010).
64. P. F. Harrison and W. G. Scott, Phys. Lett. B **594**, 324 (2004).
65. C. S. Lam, Phys. Lett. B **640**, 260 (2006).
66. R. R. Gautam and S. Kumar, Phys. Rev. D **94**, 036004 (2016).
67. K. S. Channey and S. Kumar, J. Phys. G: Nucl. Part. Phys. **46**, 015001 (2019).
68. S. Verma and M. Kashav, arXiv:1910.04467v2 (Jan. 2020).
69. A. Levitin and M. Levitin “Algorithmic Puzzles”, Oxford University Press New York (2011).

14 *Yuta Hyodo*

70. C. Hagedron and W. Rodejohann, J. High Energy Phys. **07**, 034 (2005).
71. B. Pontecorvo, Sov. Phys. JETP **6** (1957) 429.
72. B. Pontecorvo, Sov. Phys. JETP **7** (1958) 172;
73. Z. Maki, M. Nakagawa and S. Sakata, Prog. Theor. Phys. **28**, 870 (1962).
74. M. Tanabashi *et al.* (Particle Data Group), Phys. Rev. D **98**, 030001 (2018).
75. I. Esteban, M. C. Gonzalez-Garcia, A. H-Cabezudo, M. Maltoni, and T. Schwetz, J. High Energy Phys. **01**, 106 (2019). See also, NuFIT webpage, <http://www.nu-fit.org>.
76. N. Aghanim, et al. (Planck Collaboration), “Planck 2018 results. VI. Cosmological parameters”, arXiv:1807.06209v2 (Sep 2019).
77. E. Giusarma, M. Gerbino, O. Mena, S. Vagnozzi, S. Ho and K. Freese, Phys. Rev. D **94**, 083522 (2016).
78. S. Vagnozzi, E. Giusarma, O. Mena, K. Freese, M. Gerbino, S. Ho and M. Lattanzi, Phys. Rev. D **96**, 123503 (2017).
79. E. Giusarma, S. Vagnozzi, S. Ho, S. Ferraro, K. Freese, R. K.-Rubio and K.-B. Luk, Phys. Rev. D **98**, 123536 (2018).
80. M. Agostini, et al., (GERDA Collaboration), Science **365**, 1445 (2019).
81. P. F. de Salas, D. V. Forero, C. A. Ternes, Tórtola and J.W.F. Valle, Phys. Lett. B **782**, 633 (2018).
82. M. G. Aartsen, et al., (IceCube-Gen2 Collaboration) and T. J. C. Bezerra, et al., (JUNO Collaboration), Phys. Rev. D **101**, 032006 (2020).